

Received July 1, 2018, accepted August 3, 2018, date of publication August 8, 2018, date of current version August 28, 2018.

Digital Object Identifier 10.1109/ACCESS.2018.2864303

A Grey Wolf Optimizer for Optimum Parameters of Multiple PI Controllers of a Grid-Connected PMSG Driven by Variable Speed Wind Turbine

MOHAMMED H. QAIS¹, HANY M. HASANIEN², AND SAAD ALGHUWAINEM¹

¹Electrical Engineering Department, King Saud University, Riyadh 11421, Saudi Arabia

²Electrical Power and Machines Department, Ain Shams University, Cairo 11517, Egypt

Corresponding author: Mohammed H. Qais (mqais@ksu.edu.sa)

This work was supported by the Deanship of Scientific Research, College of Engineering Research Center, King Saud University, Riyadh, Saudi Arabia.

ABSTRACT This paper presents a novel application of a grey wolf optimizer (GWO) to improve the low voltage ride through (LVRT) capability and the maximum power point tracking (MPPT) of a grid-connected permanent-magnet synchronous generator driven directly by a variable-speed wind turbine (DD-PMSG-VSWT). The LVRT capability and MPPT enhancements are achieved by the optimal tuning of eight proportional-integral (PI) controllers in the cascaded control of the machine-side converter and the grid-side inverter, simultaneously. An online optimization is used and achieved by minimizing the integral-squared error of the error inputs of the PI controllers that are controlling dc link voltage, generated real power, and terminal voltages of the PMSG and the grid. The symmetrical and asymmetrical faults for testing the optimum gain parameters are simulated and examined using PSCAD/EMTDC. The obtained results of the optimum values of the GWO algorithm are compared with those attained using the optimum values of the genetic algorithm and the simplex method.

INDEX TERMS Grey wolf optimizer, permanent magnet synchronous generator, proportional integral controller, grid-connection, wind turbine.

I. INTRODUCTION

Wind power farms are being installed all over the world at an exponentially increasing rate. At least 50 GW wind power is installed in 2016 alone and is expected to be installed annually [1]. Price steadiness of wind power makes it competitive and attractive alternative to other renewable power sources. Due to the recent increase of wind power plants (WPPs) penetrations into the grid, transmission system operators (TSO) established further grid regulations to assure stable and reliable performance of electric networks [2]. The recently released regulations affirmed that WPPs must participate to the power system quality at steady state (frequency and voltage variations) and low voltage ride through (LVRT) during transient state [3], [4].

Wind turbines are categorized corresponding to the speed variation (fixed or variable), drive-train (direct-drive (DD) or indirect (gearbox)), and generator (synchronous or asynchronous). Variable-speed wind turbines (VSWTs) are better suited for capturing greater power than fixed speed

wind turbines. The merits of DD-train are less mechanical stresses and losses. On the other hand, DD-train means low rotation speed, which requires a generator with a large number of rotor poles. Permanent magnet synchronous generator (PMSG) is the most suitable generator for a low-speed direct drive because of the large number of rotor-pole-pairs. PMSG-VSWT is tied into the electrical network across the frequency converter, which contains a machine-side-converter (MSC) connected to a grid-side-inverter (GSI) through a direct current (DC) link capacitor.

Vector control is generally utilized to control the MSC and GSI, using many controllers such as: conventional proportional plus integral (PI) controllers, Fuzzy logic [5], slide mode control [6], port-controlled Hamiltonian system [7], Wavelet neural network [8], and Feedback linearization [9], etc. However, the good experience and complex computations limit the application of some controllers in the industry. PI regulators are still the widest spread controllers in the industry due to their robustness and ability and wide-range

stability margins. However, PI controllers are sensitive to elements changes and system nonlinearity. Therefore, optimal fine-tuning of PI controllers is the cheapest and most suitable solution in control system of grid-connected renewable power generation.

Many conventional and statistical methods for example Response-surface method (RSM) [10], Taguchi technique [11], Affine projection algorithm [12], and artificial neural network (ANN) [13] are used for fine tuning the gain factors of PI regulators employed in the regulator system of different power system applications. However, these methods depend on the initial values, then meta-heuristic algorithms such as cuckoo search algorithm (CSA) [14], Particle Swarm Optimization (PSO) [15], [16], gravitational search algorithm [17], Bee algorithm [18], and differential evolution algorithm [19] are competitive options for fine-tuning the parameters of PI controllers.

One of the most recently developed meta-heuristic algorithms is the Grey Wolf Optimizer (GWO) algorithm, which imitates the grey wolf community hierarchy and hunting mechanisms [20]. GWO is a simple and easy algorithm to be applied in many applications due to the decreased amount of entities. GWO algorithm is applied for load frequency control [21], the optimum flow of actual and reactive power [22], [23], the optimum size of energy storing [24], and optimum fuzzy logic systems [25].

In the previous work, we introduced a new improvement to the GWO algorithm and made a simple test on the grid-connected PMSG-VSWT for the new improvement and the original GWO with a comparison to the PSO algorithm [26]. In this paper, the GWO algorithm, simplex method, and genetic algorithm (GA) are applied for optimal tuning of gain factors of PI regulators used in the vector control of MSC and GSI of grid-connected DD-PMSG-VSWT. The objective of this study is to achieve the MPPT and improve the steady state and the LVRT capability of grid-connected DD-PMSG-VSWT. Due to the nonlinearity of the modeled system, the summation of integral squared errors (ISE) of the DC link voltage, produced power, root mean square (RMS) voltage at the machine side, and RMS voltage at the point of common coupling (PCC) between GSI and grid, is used as a fitness function. Each cascaded control of the MSC and the GSI contains four PI controllers, which results in eight PI controllers. Therefore, sixteen parameters should be optimized for better MPPT and LVRT capability. By comparing the obtained results of the GWO, the simplex, and the GA algorithms, the GWO provided the minimum ISE and hence better MPPT and LVRT capability performances.

II. POWER SYSTEM MODEL

In this study, the power system model shown in Fig. 1 is used. The model consists of the wind turbine model, drive train model, PMSG model, MSC, DC link capacitor, Chopper circuit [27], GSI, inductive and capacitive (LC) filter [28], a step up three-phase transformer, double circuit transmission lines, and the power grid.

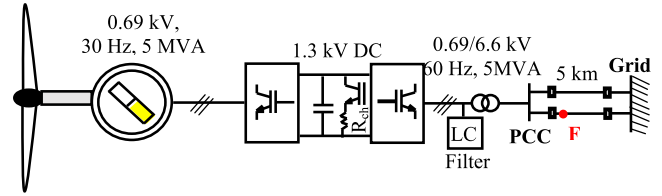


FIGURE 1. Power system model.

A. WIND TURBINE MODEL

Wind turbines convert the wind power into mechanical power (P_m) as in (1) [29]–[31]

$$P_m = 0.5\rho C_p(\lambda, \beta)Av^3 \quad (1)$$

$$C_p(\lambda, \beta) = 0.73 \left(\frac{151}{\lambda_i} - 0.58\beta - 0.002\beta^{2.14} - 13.2 \right) e^{-\frac{18.4}{\lambda_i}} \quad (2)$$

$$\frac{1}{\lambda_i} = \frac{1}{\lambda + 0.02\beta} - \frac{0.03}{1 + \beta^3} \quad (3)$$

$$\lambda = \frac{R\omega_m}{v} \quad (4)$$

$$P_{\max} = \frac{1}{2}\rho A \left(\frac{\omega_m R}{\lambda_{opt}} \right)^3 C_{Popt} \quad (5)$$

where C_p is a power coefficient which is function of the pitch angle β and the tip speed ratio (TSR) λ , ρ is the atmosphere density, the radius of blades and its area are R and A , and the wind velocity is v . The optimum parameters for maximum power (P_{\max}) are λ_{opt} and C_{Popt} .

B. MODELING OF PMSG

The terminal voltages of PMSG are written in the d-q axis as follows [32]–[34]

$$\begin{pmatrix} v_{sd} \\ v_{sq} \end{pmatrix} = -R_s \begin{pmatrix} i_{sd} \\ i_{sq} \end{pmatrix} - \frac{d}{dt} \begin{pmatrix} L_d i_{sd} \\ L_q i_{sq} \end{pmatrix} + \omega_e \begin{pmatrix} -L_q i_{sq} \\ L_d i_{sd} + \psi_f \end{pmatrix} \quad (6)$$

where the d-q voltages and currents at generator terminal are v_{sd} , v_{sq} , i_{sd} , and i_{sq} . The inductances and resistance are L_d and L_q , and R_s . the magnetic flux that linkage the stator windings is ψ_f . The mathematical model of the direct-drive train of the PMSG-VSWT is considered a single-mass shaft model since it tied to the grid across the full-scale frequency converter as follows

$$j \frac{d\omega_m}{dt} + D\omega_m = T_m - T_e \quad (7)$$

$$\omega_e = \frac{P}{2}\omega_m \quad (8)$$

where the mechanical and electrical torques are T_m and T_e . The generator inertia is j and the electrical and mechanical speed are ω_e and ω_m . The coefficient of rotor damping is D and P is the number of poles.

III. FREQUENCY CONVERTER CONTROL

The frequency converter is a back-to-back two-level voltage source converter (VSC). Each VSC is composed of six

insulated-gate bipolar transistors (IGBT) switches bypassed by anti-parallel diodes. The IGBTs are driven by pulse width modulation (PWM) produced by the cascaded controllers of the MSC and the GSI sides.

A. MSC CONTROL

The vector control of the machine (PMSG) side converter is flux oriented control, where the active power with reference P_{max} is controlled by controlling the q -axis current and voltage, and the RMS terminal generator voltage with reference 1 per unit (pu) is controlled by controlling the d -axis current and voltage, as shown in Fig. 2 [35]. Four PI controllers are used in the cascaded control of MSC, which means eight gain parameters.

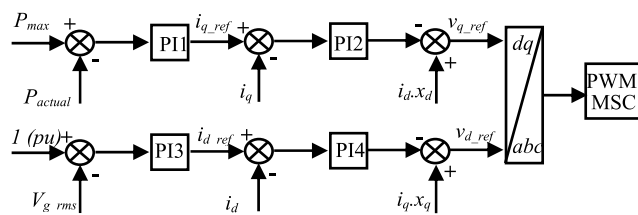


FIGURE 2. The cascaded control system of MSC side.

B. GSI CONTROL

The vector control of GSI is voltage oriented control, where the dn -axis current and voltage are regulating the DC voltage, and the qn -axis current and voltage are regulating the RMS voltage of PCC, as shown in Fig. 3. Four PI controllers are used in the cascaded control of GSI, which means eight gain parameters.

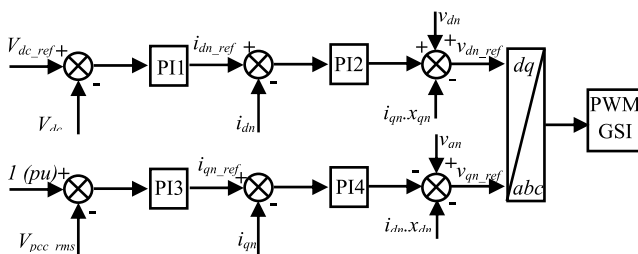


FIGURE 3. The cascaded control system of GSI side.

IV. OPTIMIZATION PROCEDURE

In this work, the GWO algorithm is written in FORTRAN and applied in PSCAD/EMTDC for online optimization. Eight PI controllers, which are shown in Fig. 2 and 3, have sixteen gain factors (proportional gains K_p and integral time constants T_i). The simplex and the GA algorithms are built in the master library of PSCAD and employed for online optimization to the model system. The main reason for the optimization is to improve the LVRT ability of WPPs that are connected to the grid. The severest fault event (three-phase-to-ground (3LG) fault) is applied, where the symmetrical fault is incepted at

position (F) in the transmission line (TL) shown in Fig. 1. The ratings' data of the simulated model are clearly labeled in Fig. 1. The capacitance of the DC stage is $80000 \mu F$ and the braking resistor is 0.5Ω . The inductance and capacitance of the LC filter are $200 \mu H$ and $200 \mu F$. The cost function is the sum of ISE as follows:

$$fitness = \sum ISE = \int (P_{max} - P_g)^2 dt + \int (1 - V_{grms})^2 dt + \int (1 - V_{dc})^2 dt + \int (1 - V_{rms_PCC})^2 dt \quad (9)$$

where P_g is the power of PMSG, P_{max} is the maximum power, V_{grms} is the generator voltage, V_{dc} is the DC voltage, and V_{rms_PCC} is RMS voltage at PCC.

For GWO and GA, the gain factor K_p is limited between [0.5, 5] and T_i is limited between [0.001, 2]. For the simplex method, the initial values are selected based on perturbing and observing method. The initial values of K_p in outer and inner loops are 2 and 1, respectively and the initial values of T_i in the outer and inner loops are 0.4 and 0.02, respectively. The appropriate selection of initial step size is very important in simplex methods and is set to 2.

A. GWO ALGORITHM

The GWO is a meta-heuristic algorithm proposed by Mirjalili et al. [20] in 2014, which imitates the social manners of grey wolves. These wolves live in a group contains 5-12 members. In this group, the strict dominance hierarchy is practiced where the group has a leader named alpha (α), supported by secondary ones named beta (β), which aid α in decision-making. The rest members of the group are named δ and ω as shown in Fig. 4.

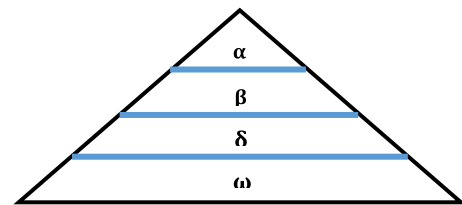


FIGURE 4. Grey wolf hierarchy.

The procedure of hunting the food by the grey wolves is: looking for the food, surrounding the food, hunting, and attacking the food. The arithmetic model of surrounding the food is written as follows

$$\vec{D} = \left| \vec{C} \cdot \vec{X}_{pi} - \vec{X}_i \right| \quad (10)$$

$$\vec{X}_{i+1} = \vec{X}_{pi} - \vec{A} \cdot \vec{D} \quad (11)$$

where X_i is the place of the grey wolf, X_{pi} is the place of the food, D is the distance, A and C are vectors calculated as following

$$\vec{a} = 2 - 2 \times t / Max_iter \quad (12)$$

$$\vec{A} = 2\vec{a} \cdot \vec{r}_1 - \vec{a} \quad (13)$$

$$\vec{C} = 2 \cdot \vec{r}_2 \quad (14)$$

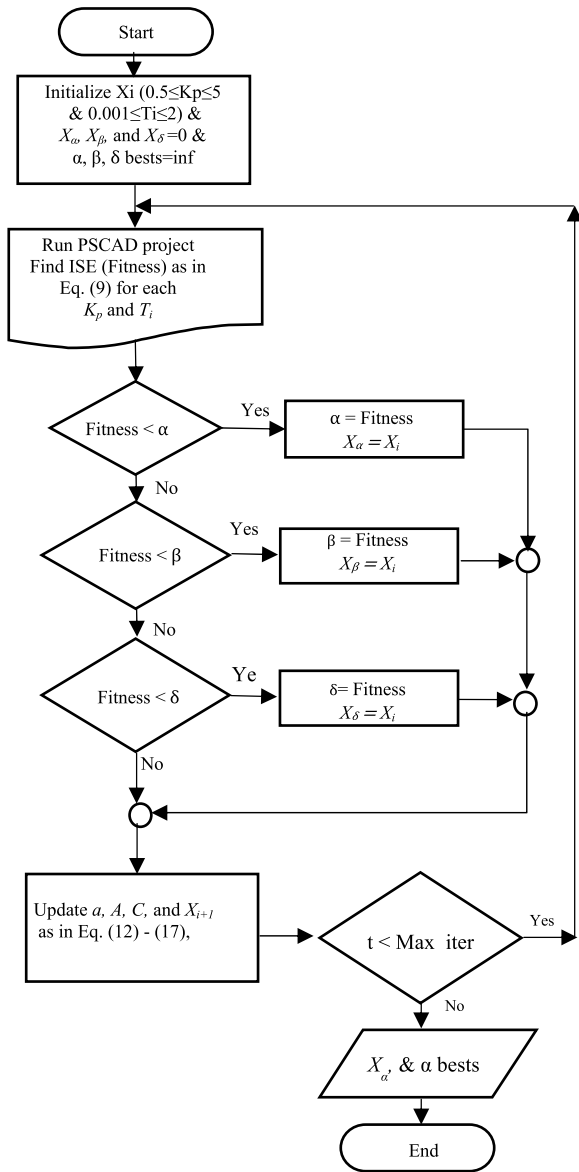


FIGURE 5. Flowchart of the GWO algorithm.

where r_1 and r_2 are random numbers between $[0, 1]$. The parameter a is a variable which is linearly reduced from 2 to 0 while the iterations increased. The process of looking for the food position (exploration) could be attained by diverging the search entities, when $|A| > 1$. The process of getting the food (exploitation) could be attained by the convergence of the search entities, when $|A| < 1$. The hunting is led by α entities with β and δ entities support as in (15)-(17). Fig.5 shows the flowchart of the GWO algorithm. Like other meta-heuristic algorithms, The GWO algorithm can be disposed to stagnate in a local minimum but the parameters A and C can help the GWO algorithm to avoid stagnation.

$$\begin{aligned} \vec{D}_\alpha &= \left| \vec{C}_1 \cdot \vec{X}_{\alpha i} - \vec{X}_i \right|, & \vec{D}_\beta &= \left| \vec{C}_2 \cdot \vec{X}_{\beta i} - \vec{X}_i \right|, \\ \vec{D}_\delta &= \left| \vec{C}_3 \cdot \vec{X}_{\delta i} - \vec{X}_i \right| \end{aligned} \quad (15)$$

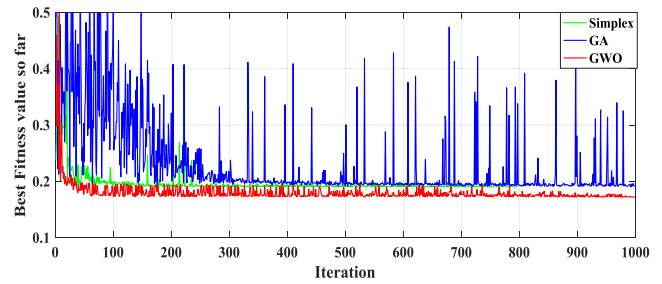


FIGURE 6. Fitness value for 1000 multiple PSCAD runs.

TABLE 1. Fitness values.

Algorithm	ISE
Simplex	0.190367
GA	0.189789
GWO	0.171859

$$\begin{aligned} \vec{X}_1 &= \vec{X}_{\alpha i} - \vec{A}_1 \cdot \vec{D}_\alpha, & \vec{X}_2 &= \vec{X}_{\beta i} - \vec{A}_2 \cdot \vec{D}_\beta, \\ \vec{X}_3 &= \vec{X}_{\delta i} - \vec{A}_3 \cdot \vec{D}_\delta \end{aligned} \quad (16)$$

$$\vec{X}_{i+1} = \frac{\vec{X}_1 + \vec{X}_2 + \vec{X}_3}{3} \quad (17)$$

B. SIMPLEX SEARCH METHOD

The simplex search algorithm, which is derivative-free and a very simple direct approach for unconstrained optimization of deterministic functions, was proposed by Nelder and Mead [36]. However, the initial values settings play an important role in finding the optimum solution and will not guarantee the global optima. The initial values of gain parameters and the initial step size should be selected carefully. Four operations are used reflection, expansion, contraction, and shrink as in (18)-(21).

$$\vec{X}_{ref} = (1 + \alpha)\vec{X}_{cent} - \alpha\vec{X}_{n+1} \quad (18)$$

$$\vec{X}_{exp} = (1 - \gamma)\vec{X}_{cent} + \gamma\vec{X}_{ref} \quad (19)$$

$$\vec{X}_{cont} = (1 - \beta)\vec{X}_{cent} + \beta\vec{X}_{n+1} \quad (20)$$

$$\vec{X}_i = (1 - \delta)\vec{X}_1 + \delta\vec{X}_i \quad (21)$$

where X_{ref} , X_{exp} , X_{cont} , and X_i are reflected, expanded, contracted, and shrink points, respectively. α , γ , β and δ are reflection, expansion, contraction, and shrink coefficients which equal 1, 2, 0.5, and 0.5 respectively.

C. GENETIC ALGORITHM (GA)

The GA is an evolutionary metaheuristic algorithm which has been applied to many power system control optimization [37], [38]. GAs work with a population of entities denoted by bit strings and change the population with random exploration and competition. In general, GAs consist of trials for example generation, crossover, and mutation. Generation is a procedure in which a novel cluster of entities is made by choosing the proper entities in the existing population.

TABLE 2. Optimal gain factors of PI controllers (MSC).

		Simplex	GA	GWO
PI1	K_p	2.5029	3.545295	1.796658
	T_i	2.21E-03	8.35E-03	0.002603
PI2	K_p	2.443623	3.51955	5
	T_i	1.193722	0.963056	0.193508
PI3	K_p	1.508484	3.545295	1.273237
	T_i	0.240437	0.00835	0.38853
PI4	K_p	1.43067	3.51955	0.875182
	T_i	0.511124	0.963056	0.21366

TABLE 3. Optimal gain factors of PI controllers (GSI).

		Simplex	GA	GWO
PI1	K_p	1.56183	0.645102	0.538597
	T_i	0.420939	0.635668	0.007046
PI2	K_p	1.666144	0.625844	1.271061
	T_i	0.597861	0.32668	1.663751
PI3	K_p	0.713904	0.645102	0.53383
	T_i	0.384169	0.635668	0.043766
PI4	K_p	0.875751	0.625844	1.793417
	T_i	0.447672	0.32668	0.145899

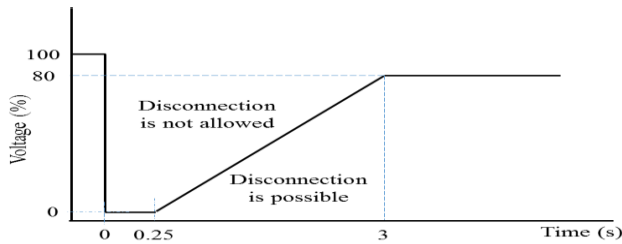


FIGURE 7. The combined form of LVRT capability.

TABLE 4. System stability at different TL inductance.

	GWO	GA	Simplex
+50% of L_{TL}	Stable	Stable	Unstable
-50% of L_{TL}	Stable	Stable	Stable

Crossover is the greatest influential worker in GAs. It constructs novel children by choosing two strings and exchange segments of their structures. The novel children may interchange the worst entities in the population. Mutation is a local worker with a very low likelihood. Its purpose is to adjust the value of a random position in a string.

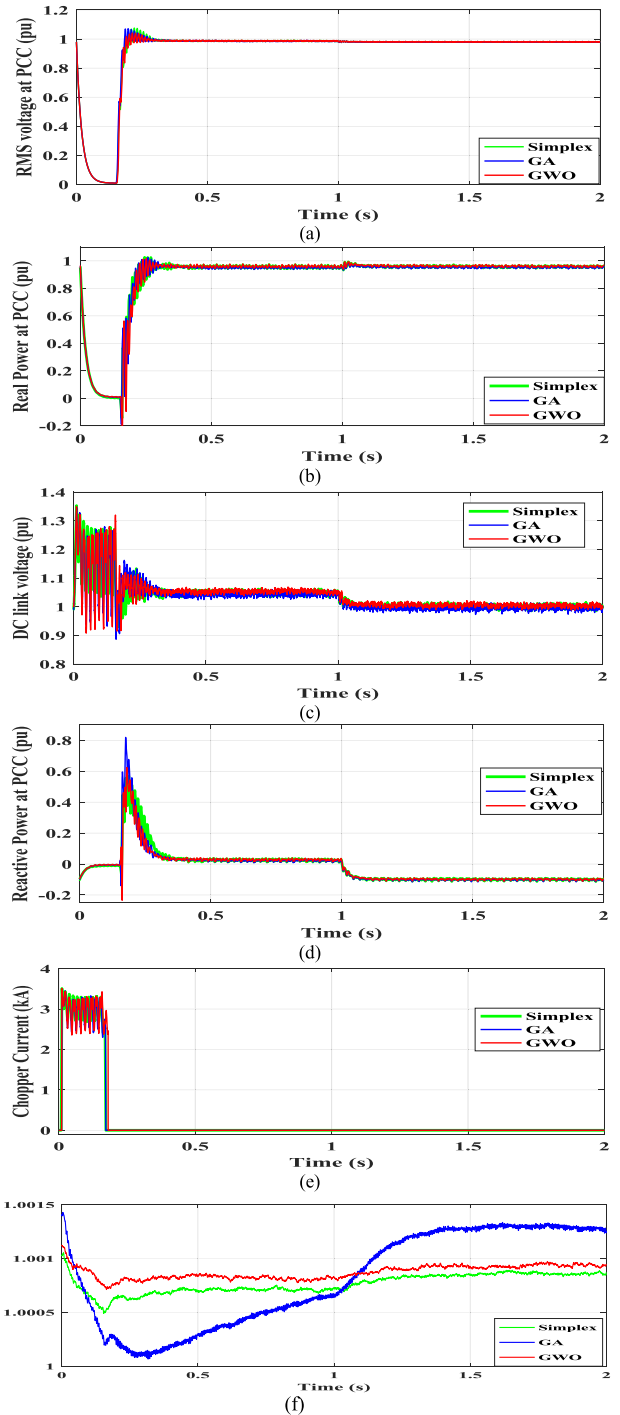


FIGURE 8. Responses for 3LG Fault with successful reclosed CBs. (a) PCC RMS voltage. (b) Actual power at PCC. (c) DC voltage. (d) Reactive power at PCC. (e) Chopper current. (f) Rotor speed of PMSG.

D. OPTIMIZATION RESULTS

The optimization is attained by finding the minimum of the cost function shown in (9). The iteration number of PSCAD project is 1000 iterations and the period of each iteration is 10 sec. For the simplex method, the tolerance is 0.000001,

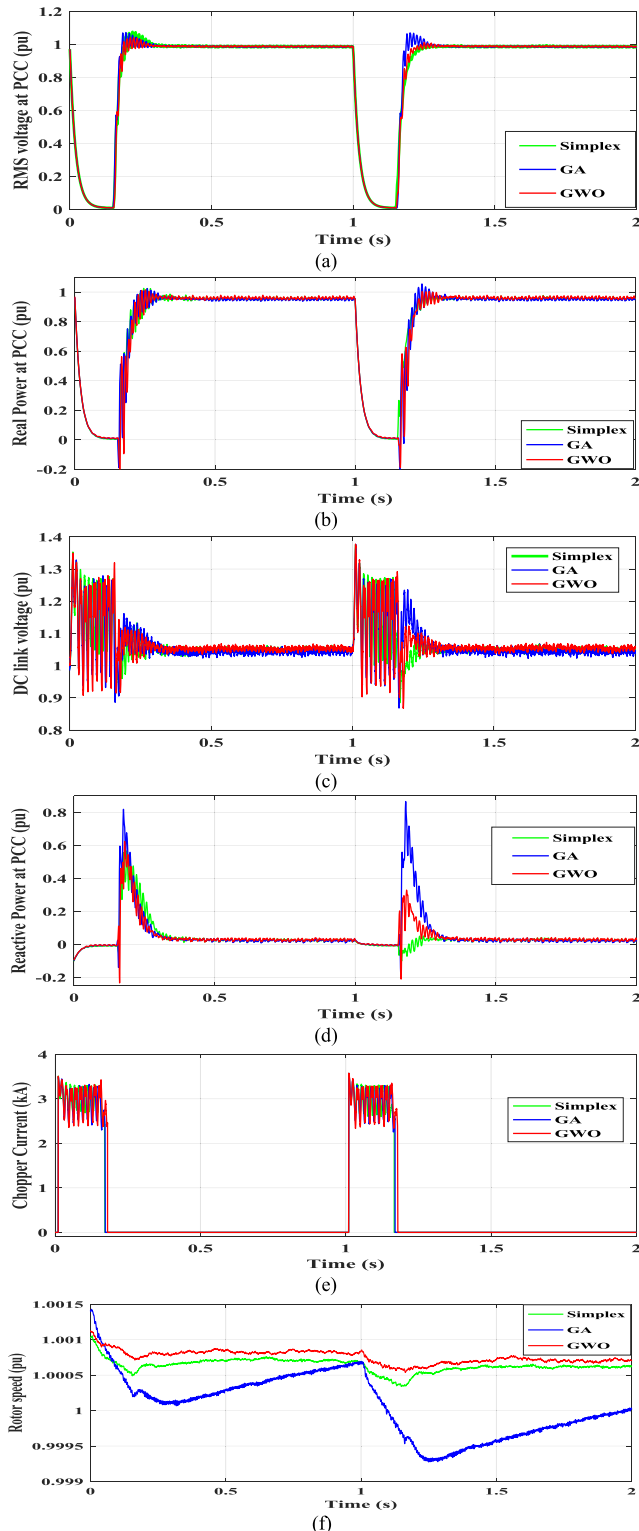


FIGURE 9. Responses for permanent 3LG Fault with unsuccessful reclosed CBs. (a) PCC RMS voltage. (b) Actual power at PCC. (c) DC voltage. (d) Reactive power at PCC. (e) Rotor speed of PMSG.

then the optimization stopped at 792 runs. Fig. 6 shows the optimization performance using the simplex method, the genetic algorithm, and the GWO algorithm. It is clear that

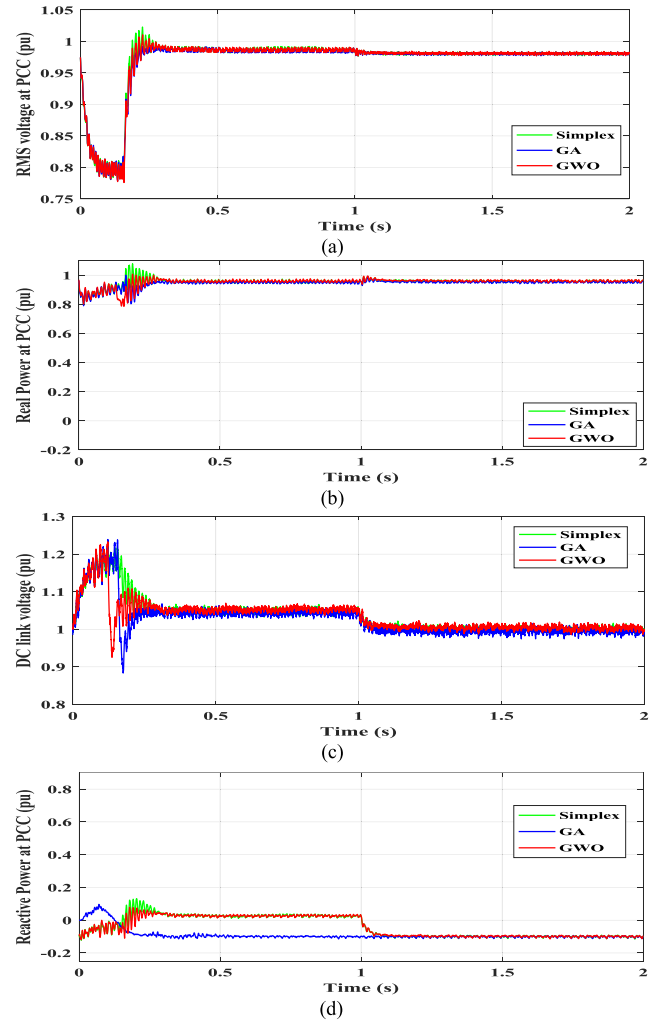


FIGURE 10. Responses for 1LG Fault with successful reclosed CBs. (a) PCC RMS voltage. (b) Actual power at PCC. (c) DC voltage. (d) Reactive power at PCC.

the GWO converged to the minimum faster than the other methods. Table 1 shows the fitness values (minimum ISE), where the minimum one is achieved by the GWO algorithm. The optimum 16 gain parameters of eight PI controllers are shown in Table 2 and 3.

V. SIMULATION RESULTS

The optimum gain parameters were applied to the power system model shown in Fig. 1, which is simulated using PSCAD/EMTDC. The time step setting is 20 μ s and the fault duration time is 0.15 s. Due to the short time of transient cases, it is assumed that the wind speed is unvarying. The MPPT, the steady state, and LVRT capability are tested for the GWO algorithm and compared to the genetic algorithm and simplex method. Many grid codes presented for LVRT capability, the combined form of all grid codes is presented in Fig. 7 [4]. The LVRT capability is tested when the symmetrical and asymmetrical faults occurred in one TL of the two-circuit TLs at the location (F), as shown in Fig. 1.

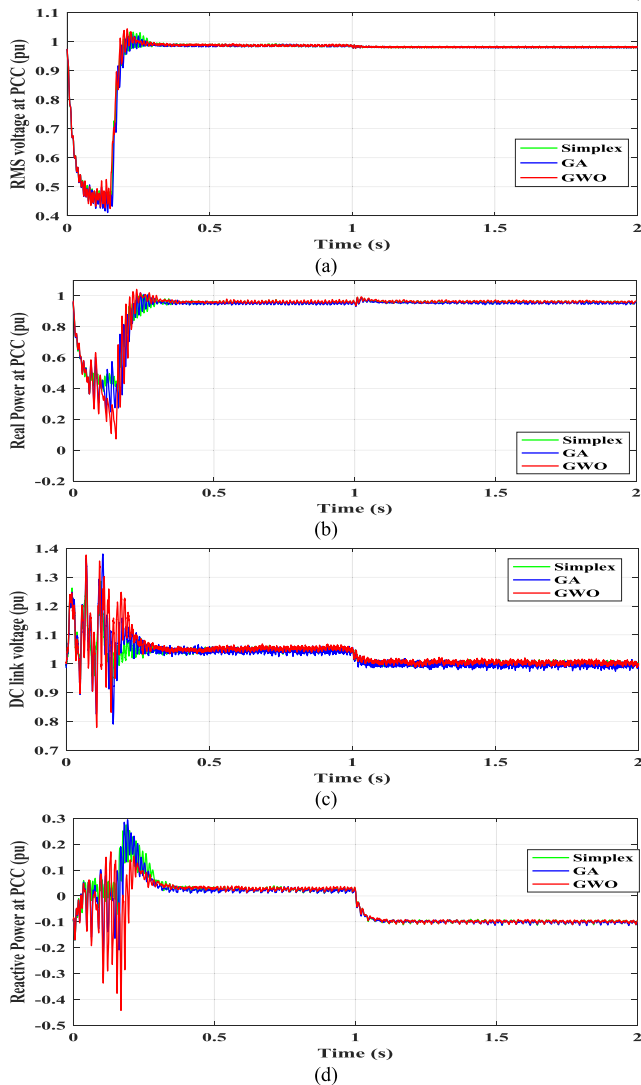


FIGURE 11. Responses to 2LG Fault with successful reclosed CBs. (a) PCC RMS voltage. (b) Actual power at PCC. (c) DC voltage. (d) Reactive power at PCC.

The faulted TL is tripped after 0.15s and after 0.85s the CBs are auto-reclosed after the fault clearance (e.g. flashover or arc is distinguished). On the other hand, the system stability when using optimum parameters is tested with a 50% increase or a decrease of TL inductance (L_{TL}) as shown in Table 4.

A. SYMMETRICAL FAULTS

The symmetrical three-line-to-ground (3LG) fault is the worst type of fault that can occur in the power system. The optimum gain parameters, which are obtained by the GWO algorithm, the GA algorithm, and the Simplex method, are tested during 3LG fault with successful and unsuccessful reclosing of circuit breakers (CBs). The overshoot and steady state error of the terminal voltage and the actual power response using the GWO algorithm are much better compared to those using the GA and the simplex methods as

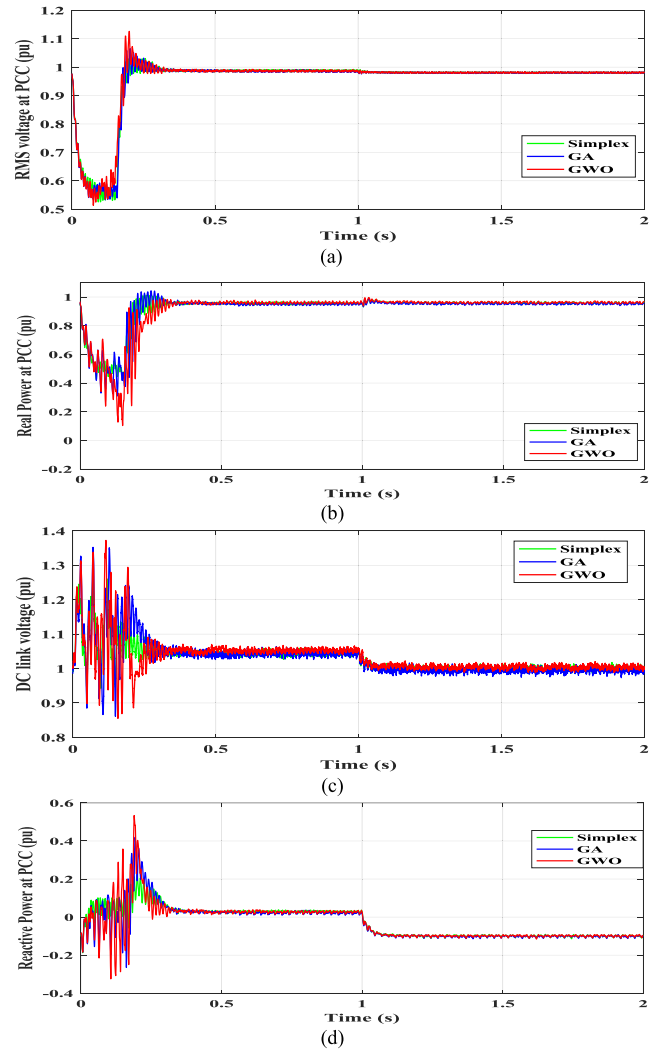


FIGURE 12. Responses to L-L Fault with successful reclosed CBs. (a) PCC RMS voltage. (b) Actual power at PCC. (c) DC voltage. (d) Reactive power at PCC.

shown in Figs. 8-(a), 8-(b), 9-(a), and 9-(b). The MPPT supplied more power when the GWO algorithm used as shown in Figs. 8-(b) and 9-(b). The DC link voltage response is smoother when using the GWO compared to the GA and the simplex algorithm as shown in Figs. 8-(c) and 9-(c). The required reactive power support for voltage recovery is less when using the GWO compared to the GA as shown in Figs. 8-(d) and 9-(d). The Chopper current during the fault for the GWO, GA, and Simplex algorithms is displayed in Fig. 8-(e). The response curve of rotor-speed is robust when using the GWO algorithm in contrast with that of using the GA algorithm as shown in Figs. 8-(f) and 9-(f).

B. ASYMMETRICAL FAULTS

The optimum gain parameters are tested during single-line-to-ground (1LG) fault, line-to-line-to-ground (2LG) fault, and line-to-line (LL) fault as shown in Figs. 10-12. For 1LG fault, the response of the RMS voltage and real

power when using the GWO algorithm and GA algorithm is better when using the simplex method as shown in Figs. 10-(a) and 10-(b). The response of DC link is much better for the simplex method compared to the GWO and GA algorithm as shown in Fig. 10-(c). The reactive power support using simplex is greater than GWO and GA as shown in Fig. 10-(d). For 2LG fault, the response of the RMS voltage, the actual power, the DC link, and the reactive power has no difference between the applied algorithms as shown in Figs. 11-(a)-(d). For L-L fault, the response of RMS voltage for the GWO algorithm has bigger overshoot compared to the responses of GA and simplex as shown in Fig. 12-(a). The overshoot of the actual power response when using the GA is bigger than the GWO algorithm as shown in Fig. 12-(b). Figs. 12-(c) and 12-(d) show no big difference in the DC link voltage and reactive power responses using the GWO and the GA algorithms.

VI. CONCLUSION

In this paper, the LVRT capability, the MPPT, and the steady-state operation of grid-connected DD-PMSG-VSWT are enhanced by determining the optimal gain factors of PI regulators used in the control schemes of MSC and GSI. The GWO algorithm, GA algorithm, and Simplex method are used to achieve the optimum gain factors by finding the minima of the summation of integral-squared-error of DC voltage error, produced real power error, and terminal voltage errors of PMSG and the grid. It is found that the GWO algorithm provides the best convergence to the minimum value and better response of the MPPT and the LVRT capability during symmetrical and asymmetrical faults. The GA algorithm provides the worst rotor speed response during all fault types. The simplex method provides reasonable response due to the help of initial inputs. In addition to the previous successful employment of the GWO in different electrical power system optimization areas, it can be concluded that the GWO algorithm is a competitive meta-heuristic algorithm to tune many PI regulators in a grid-connected DD-PMSG-VSWT.

REFERENCES

- [1] GWEC. (2017). *Global Wind Report 2016*. Accessed: Dec. 1, 2017. [Online]. Available: <http://gvec.net/publications/global-wind-report-2/>
- [2] M. Tsili and S. Papathanassiou, "A review of grid code technical requirements for wind farms," *IET Renew. Power Gener.*, vol. 3, no. 3, pp. 308–332, Sep. 2009.
- [3] X. Liu, Z. Xu, and K. P. Wong, "Recent advancement on technical requirements for grid integration of wind power," *J. Mod. Power Syst. Clean Energy*, vol. 1, no. 3, pp. 216–222, 2013.
- [4] A. M. Howlader and T. Senjyu, "A comprehensive review of low voltage ride through capability strategies for the wind energy conversion systems," *Renew. Sustain. Energy Rev.*, vol. 56, pp. 643–658, Apr. 2016.
- [5] A. Beddar, H. Bouzekri, B. Babes, and H. Afghoul, "Experimental enhancement of fuzzy fractional order PI+I controller of grid connected variable speed wind energy conversion system," *Energy Convers. Manage.*, vol. 123, pp. 569–580, Sep. 2016.
- [6] Z. Li, C. Zang, P. Zeng, H. Yu, S. Li, and J. Bian, "Control of a grid-forming inverter based on sliding-mode and mixed H_2/H_∞ control," *IEEE Trans. Ind. Electron.*, vol. 64, no. 5, pp. 3862–3872, May 2017.
- [7] Y. Gui, C. Kim, and C. C. Chung, "Improved low-voltage ride through capability for PMSG wind turbine based on port-controlled hamiltonian system," *Int. J. Control, Automat. Syst.*, vol. 14, no. 5, pp. 1195–1204, 2016.
- [8] M. Alizadeh and S. S. Kojori, "Augmenting effectiveness of control loops of a PMSG (permanent magnet synchronous generator) based wind energy conversion system by a virtually adaptive PI (proportional integral) controller," *Energy*, vol. 91, pp. 610–629, Nov. 2015.
- [9] Y. Errami, M. Ouassaid, and M. Maaroufi, "A performance comparison of a nonlinear and a linear control for grid connected PMSG wind energy conversion system," *Int. J. Elect. Power Energy Syst.*, vol. 68, pp. 180–194, Jun. 2015.
- [10] H. M. Hasanien and S. M. Muyeen, "Design optimization of controller parameters used in variable speed wind energy conversion system by genetic algorithms," *IEEE Trans. Sustain. Energy*, vol. 3, no. 2, pp. 200–208, Apr. 2012.
- [11] H. M. Hasanien and S. M. Muyeen, "A Taguchi approach for optimum design of proportional-integral controllers in cascaded control scheme," *IEEE Trans. Power Syst.*, vol. 28, no. 2, pp. 1636–1644, May 2013.
- [12] H. M. Hasanien and S. M. Muyeen, "Affine projection algorithm based adaptive control scheme for operation of variable-speed wind generator," *IET Gener., Transmiss. Distrib.*, vol. 9, no. 16, pp. 2611–2616, 2015.
- [13] T. Pajchrowski, K. Zawirski, and K. Nowopolski, "Neural speed controller trained online by means of modified RPROP algorithm," *IEEE Trans. Ind. Inform.*, vol. 11, no. 2, pp. 560–568, Apr. 2015.
- [14] R. N. Kalaam, S. M. Muyeen, A. Al-Durra, H. M. Hasanien, and K. Al-Wahedi, "Optimisation of controller parameters for grid-tied photovoltaic system at faulty network using artificial neural network-based cuckoo search algorithm," *IET Renew. Power Gener.*, vol. 11, no. 12, pp. 1517–1526, 2017.
- [15] J. Zhao, M. Lin, D. Xu, L. Hao, and W. Zhang, "Vector control of a hybrid axial field flux-switching permanent magnet machine based on particle swarm optimization," *IEEE Trans. Magn.*, vol. 51, no. 11, Nov. 2015, Art. no. 8204004.
- [16] C. H. Liu and Y. Y. Hsu, "Design of a self-tuning PI controller for a STATCOM using particle swarm optimization," *IEEE Trans. Ind. Electron.*, vol. 57, no. 2, pp. 702–715, Feb. 2010.
- [17] R.-E. Precup, R.-C. David, E. M. Petriu, M.-B. Radac, and S. Preitl, "Adaptive GSA-based optimal tuning of PI controlled servo systems with reduced process parametric sensitivity, robust stability and controller robustness," *IEEE Trans. Cybern.*, vol. 44, no. 11, pp. 1997–2009, Nov. 2014.
- [18] B. L. G. Costa, V. D. Bacon, S. A. O. da Silva, and B. A. Angélico, "Tuning of a PI-MR controller based on differential evolution metaheuristic applied to the current control loop of a shunt-APF," *IEEE Trans. Ind. Electron.*, vol. 64, no. 6, pp. 4751–4761, Jun. 2017.
- [19] S. Mirjalili, S. M. Mirjalili, and A. Lewis, "Grey wolf optimizer," *Adv. Eng. Softw.*, vol. 69, pp. 46–61, Mar. 2014.
- [20] N. E. Y. Kouba, M. Mena, M. Hasni, and M. Boudour, "LFC enhancement concerning large wind power integration using new optimised PID controller and RFBs," *IET Gener., Transmiss. Distrib.*, vol. 10, no. 16, pp. 4065–4077, 2016.
- [21] M. H. Sulaiman, Z. Mustaffa, M. R. Mohamed, and O. Aliman, "Using the gray wolf optimizer for solving optimal reactive power dispatch problem," *Appl. Soft Comput.*, vol. 32, pp. 286–292, Jul. 2015.
- [22] A. A. El-Fergany and H. M. Hasanien, "Single and multi-objective optimal power flow using grey wolf optimizer and differential evolution algorithms," *Electr. Power Compon. Syst.*, vol. 43, no. 13, pp. 1548–1559, Aug. 2015.
- [23] A. Fathy and A. Y. Abdelaziz, "Grey wolf optimizer for optimal sizing and siting of energy storage system in electric distribution network," *Electr. Power Compon. Syst.*, vol. 45, no. 6, pp. 601–614, Apr. 2017.
- [24] R. E. Precup, R. C. David, and E. M. Petriu, "Grey wolf optimizer algorithm-based tuning of fuzzy control systems with reduced parametric sensitivity," *IEEE Trans. Ind. Electron.*, vol. 64, no. 1, pp. 527–534, Jan. 2017.
- [25] M. H. Qais, H. M. Hasanien, and S. Alghuwainem, "Augmented grey wolf optimizer for grid-connected PMSG-based wind energy conversion systems," *Appl. Soft Comput.*, vol. 69, pp. 504–515, Aug. 2018.
- [26] N. A. Orlando, M. Liserre, R. A. Mastromauro, and A. Dell'Aquila, "A survey of control issues in PMSG-based small wind-turbine systems," *IEEE Trans. Ind. Informat.*, vol. 9, no. 3, pp. 1211–1221, Aug. 2013.
- [27] R. Peña-Alzola, M. Liserre, F. Blaabjerg, M. Ordóñez, and Y. Yang, "LCL-filter design for robust active damping in grid-connected converters," *IEEE Trans. Ind. Informat.*, vol. 10, no. 4, pp. 2192–2203, Nov. 2014.
- [28] S. M. Muyeen, J. Tamura, and T. Murata, *Stability Augmentation of a Grid-Connected Wind Farm*. London, U.K.: Springer, 2008.
- [29] S. Heier, *Grid Integration of Wind Energy: Onshore and Offshore Conversion Systems*. Hoboken, NJ, USA: Wiley, 2014.

- [30] S. Li and J. Li, "Output predictor-based active disturbance rejection control for a wind energy conversion system with PMSG," *IEEE Access*, vol. 5, pp. 5205–5214, 2017.
- [31] O. P. Mahela and A. G. Shaik, "Comprehensive overview of grid interfaced wind energy generation systems," *Renew. Sustain. Energy Rev.*, vol. 57, pp. 260–281, May 2016.
- [32] B. Zaker, G. B. Gharehpetian, and M. Karrari, "Improving synchronous generator parameters estimation using $d - q$ axes tests and considering saturation effect," *IEEE Trans. Ind. Informat.*, vol. 14, no. 5, pp. 1898–1908, May 2018.
- [33] D. Reddy and S. Ramasamy, "Design of RBFN controller based boost type vienna rectifier for grid-tied wind energy conversion system," *IEEE Access*, vol. 6, pp. 3167–3175, 2018.
- [34] B. Wu, Y. Lang, N. Zargari, and S. Kouro, *Power Conversion and Control of Wind Energy Systems*, 1st ed. Hoboken, NJ, USA: Wiley, 2011.
- [35] J. A. Nelder and R. Mead, "A simplex method for function minimization," *Comput. J.*, vol. 7, no. 4, pp. 308–313, Jan. 1965.
- [36] M. Zhao, Z. Chen, and F. Blaabjerg, "Optimisation of electrical system for offshore wind farms via genetic algorithm," *IET Renew. Power Gener.*, vol. 3, no. 2, pp. 205–216, Jun. 2009.
- [37] H.-U. Shin and K.-B. Lee, "Optimal design of a 1 kW switched reluctance generator for wind power systems using a genetic algorithm," *IET Electr. Power Appl.*, vol. 10, no. 8, pp. 807–817, 2016.



MOHAMMED H. QAIS received the B.Sc. degree in electrical engineering from the Faculty of Engineering, Sana'a University, Sana'a, Yemen, in 2007, and the M.Sc. degree from the Faculty of Engineering, King Saud University, Riyadh, Saudi Arabia, in 2014, where he is currently pursuing the Ph.D. degree in electrical engineering. His research interests include renewable energy systems operation, control, and optimization and power system relaying and transients.



HANY M. HASANIEN received the B.Sc., M.Sc., and Ph.D. degrees in electrical engineering from the Faculty of Engineering, Ain Shams University, Cairo, Egypt, in 1999, 2004, and 2007, respectively. From 2008 to 2011, he was a Joint Researcher with the Kitami Institute of Technology, Kitami, Japan. From 2012 to 2015, he was an Associate Professor with the College of Engineering, King Saud University, Riyadh, Saudi Arabia. He is currently a Professor with the Electrical Power and Machines Department, Faculty of Engineering, Ain Shams University. He has authored, co-authored, and edited three books in the field of electric machines and renewable energy. He has published over 90 papers in international journals and conferences. His biography was included in Marquis Who's Who in the world for its 28th edition, in 2011. His research interests include modern control techniques, power systems dynamics and control, energy storage systems, renewable energy systems, and smart grid. He received the Encouraging Egypt Award for Engineering Sciences in 2012 and the Institutions Egypt Award for Invention and Innovation of Renewable Energy Systems Development in 2014. He is an Editorial Board Member of the *Electric Power Components and Systems Journal*. He is also an Associate Editor of *IET Renewable Power Generation*.



SAAD ALGHUWAINEM received the B.Sc. degree from King Saud University, Riyadh, Saudi Arabia, in 1974, the M.Sc. degree from the University of Colorado, Boulder, CO, USA, in 1978, and the Ph.D. degree from the University of Michigan, Ann Arbor, MI, USA, in 1986, all in electrical engineering. Since 1986, he has been with the Department of Electrical Engineering, King Saud University, where he is currently a Professor. His research interests include renewable energy systems operation, control and optimization, power system protection, and electromagnetic transients.

...